Chemical Science

ROYAL SOCIETY OF CHEMISTRY

EDGE ARTICLE

View Article Online
View Journal | View Issue

Cite this: *Chem. Sci.*, 2022, **13**, 5382

All publication charges for this article have been paid for by the Royal Society of Chemistry

Received 7th February 2022
Accepted 11th April 2022

DOI: 10.1039/d2sc00764a

rsc.li/chemical-science

Site-selective coupling of remote C(sp^3)–H/*meta*-C(sp^2)–H bonds enabled by Ru/photoredox dual catalysis and mechanistic studies†

Hong-Chao Liu,‡[a] Xiangtao Kong,‡[b] Xiao-Ping Gong,[a] Yuke Li,[c] Zhi-Jie Niu,[a] Xue-Ya Gou,[a] Xue-Song Li,[a] Yu-Zhao Wang,[a] Wei-Yu Shi,[a] Yan-Chong Huang,[a] Xue-Yuan Liu *[a] and Yong-Min Liang *[a]

Construction of C(sp^2)–C(sp^3) bonds *via* regioselective coupling of C(sp^2)–H/C(sp^3)–H bonds is challenging due to the low reactivity and regioselectivity of C–H bonds. Here, a novel photoinduced Ru/photocatalyst-cocatalyzed regioselective cross-dehydrogenative coupling of dual remote C–H bonds, including inert γ-C(sp^3)–H bonds in amides and *meta*-C(sp^2)–H bonds in arenes, to construct *meta*-alkylated arenes has been accomplished. This metallaphotoredox-enabled site-selective coupling between remote inert C(sp^3)–H bonds and *meta*-C(sp^2)–H bonds is characterized by its unique site-selectivity, redox-neutral conditions, broad substrate scope and wide use of late-stage functionalization of bioactive molecules. Moreover, this reaction represents a novel case of regioselective cross-dehydrogenative coupling of unactivated alkanes and arenes *via* a new catalytic process and provides a new strategy for *meta*-functionalized arenes under mild reaction conditions. Density functional theory (DFT) calculations and control experiments explained the site-selectivity and the detailed mechanism of this reaction.

Introduction

C–C bond construction is a long-standing target in organic chemistry. In recent years, construction of C–C bonds *via* cross-dehydrogenative coupling (CDC) has made great progress due to its atom- and step-economy.[1] In a pioneering study, Fagnou and co-workers reported the catalytic coupling of indole derivatives and aromatic derivatives enabled by a palladium catalyst.[2] Subsequently, various cross-dehydrogenative coupling reactions forming C(sp^2)–C(sp^2) bonds were developed.[3] However, apart from Minisci-type reactions, C(sp^2)–C(sp^3) bond construction *via* coupling of C(sp^2)–H bonds in arenes (excluding heteroaromatic rings, the same below) and C(sp^3)–H bonds in alkanes is rare. In fact, Li developed the Ru(II)-catalyzed oxidative coupling of (sp^3)–H bonds in cycloalkanes with *ortho*-(sp^2)–H bonds in 2-arylpyridines.[4] Though excellent work has been done in this field, coupling of C(sp^2)–H bonds in arenes and C(sp^3)–H bonds mainly focused on the use of simple cycloalkanes or hydrocarbons with extraordinarily reactive C(sp^3)–H bonds as alkylating agents, such as benzyl C(sp^3)–H

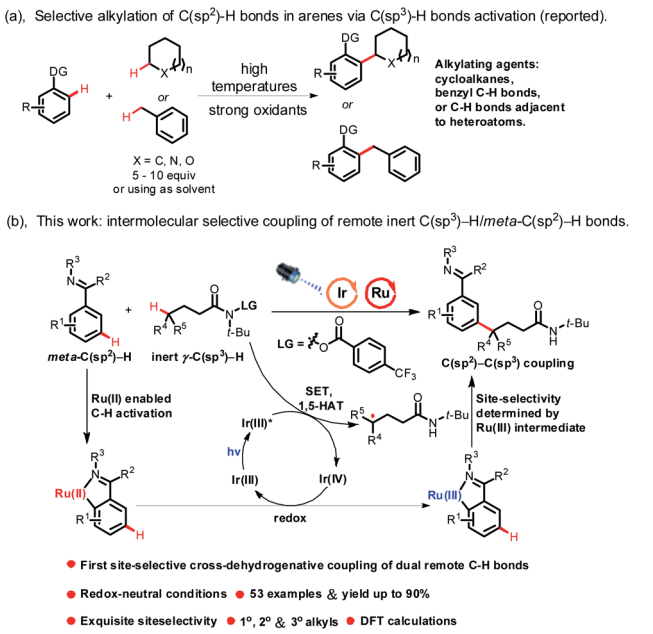

Scheme 1 (a) General coupling of C–H bond reaction modes; (b) our work.

[a]*State Key Laboratory of Applied Organic Chemistry, Lanzhou University, Lanzhou 730000, China. E-mail: liangym@lzu.edu.cn*

[b]*Henan Key Laboratory of New Optoelectronic Functional Materials, College of Chemistry and Chemical Engineering, Anyang Normal University, Anyang 455000, China*

[c]*Department of Chemistry and Centre for Scientific Modeling and Computation, Chinese University of Hong Kong, Shatin, Hong Kong, China*

† Electronic supplementary information (ESI) available. CCDC 2106363, 2105563 and 2101150. For ESI and crystallographic data in CIF or other electronic format see https://doi.org/10.1039/d2sc00764a

‡ H.-C. L. and X. K. contributed equally to this paper.

bonds and C(sp^3)–H bonds adjacent to heteroatoms (Scheme 1a),[5] and their transformations were centralized on using dangerously strong oxidants (such as peroxides) or high temperatures to enable oxidative cleavage of the C(sp^3)–H bonds to generate C(sp^3)-centered radicals, meaning that this kind of reaction suffers from limited substrate scope.[6] What's more, CDC of C(sp^2)–H bonds in arenes and unactivated C(sp^3)–H bonds (except C(sp^3)–H bonds in simple cycloalkanes, the same below) remained challenging and was difficult to achieve due to the low reactivity and regioselectivity of unactivated C(sp^3)–H bonds. In addition, alkylated arenes have found numerous applications in *inter alia* natural product synthesis, medicinal chemistry and materials science. Thus, a new methodology that could effectively construct C(sp^2)–C(sp^3) bonds *via* coupling of C(sp^2)–H bonds in arenes and unactivated C(sp^3)–H bonds with high regioselectivity under mild reaction conditions is in high demand.

The strategy of hydrogen atom transfer (HAT) has emerged as an effective tool to activate C(sp^3)–H bonds. However, activation of C(sp^3)–H bonds *via* this strategy generally lacked regioselectivity. The Hofmann–Löffler–Freytag (HLF) reaction,[7] radical translocation processes triggered by nitrogen-centered radicals, such as 1,5-hydrogen atom transfer (1,5-HAT), was well documented and has been proven to be an effective strategy for the controllable and selective functionalization of remote inert C(sp^3)–H bonds in complex molecules. Excellent work has been done in the past decades.[8] Until now, the HLF reaction has mainly focused on halogenation,[9] Michael addition,[10] Minisci reaction[11] and coupling with nucleophiles.[12] However, C-centered radical coupling with intermolecular C(sp^2)–H bonds of arenes has not been developed yet. Therefore, a method that could effectively construct C(sp^2)–C(sp^3) bonds by site-selective coupling of remote inert C(sp^3)–H bonds and C(sp^2)–H bonds in arenes would be of great importance, and by this method, remote C(sp^3)–H bond arylated products could be obtained in an atom- and step-economical approach.

Despite considerable advances in *ortho*-arene C–H bond functionalization, *meta*-arene C–H bond transformation remains elusive. The strategy of ruthenium-catalyzed σ-activation devised by Ackermann, Frost, and others is a powerful technique for *meta*-arene C–H bond transformation.[13] So far, excellent work has been done in this area, such as bromination,[14] sulfonation,[15] nitration[16] and alkylation.[17] However, *meta*-alkylation of arenes mainly focused on the use of alkyl halides as alkylating agents, and to the best of our knowledge, Ru-catalyzed *meta*-alkylation of arenes through regioselective activation of unactivated C(sp^3)–H bonds has not yet been reported, which was challenging to realize due to both the reactivity and regioselectivity needing to be simultaneously controlled in the reaction. In addition, *meta*-alkylation reactions mainly employed substrates that could produce radicals *via* single electron transfer (SET) with Ru-catalysts as alkylating agents, which severely restricted the development of *meta*-alkylation reactions. Therefore, a new methodology that could produce radicals *via* a new catalytic process rather than through SET with Ru-catalysts would expand the scope of *meta*-arene C–H bond functionalization reactions, and would provide a new synthetic platform for *meta*-functionalized arenes. Continuing our research interest in the *meta*-C(sp^2)–H bond functionalization reaction[18] and remote C(sp^3)–H bond activation reaction,[19] here we disclosed a novel example of dual Ru/photoredox-catalyzed *meta*-alkylation of arenes *via* site-selective coupling of dual remote C–H bonds, including unactivated γ-C(sp^3)–H bonds in amides and *meta*-C(sp^2)–H bonds in arenes. This reaction represents a novel example of employing a photocatalyst/Ru as a co-catalyst for regioselective CDC of unactivated alkanes and arenes *via* a new catalytic process, and provides a new strategy to synthesize *meta*-functionalized arenes under mild reaction conditions (Scheme 1b).

Results and discussion

We commenced our study using 2-phenylpyridine **1a** and *N*-(*tert*-butyl)-4-methyl-*N*-((4-(trifluoromethyl)benzoyl)oxy)pentanamide **2a** as model substrates (Table 1). With [$RuCl_2$(*p*-cymene)]$_2$/Ir(ppy)$_3$ as the cocatalyst, the desired product **3a** was obtained in 84% yield under blue LED irradiation at 60 °C after 36 h (entry 1). Further investigation disclosed that the phosphine ligand and carboxylic additive were the key to accomplishing this reaction (entries 2 and 3). It is noteworthy that Ir(ppy)$_3$ is of great importance in this reaction, as other photocatalysts, such as 4CzIPN, Ir[dF(CF_3)ppy]$_2$(dtbbpy)PF_6 and Eosin, failed to trigger the coupling reaction (entries 4–6). Variation in other solvents fell short of 1,4-dioxane (entries 7–10). The Ru-catalyst was also investigated, and the results indicated that [$RuCl_2$(*p*-cymene)]$_2$ was more efficient than the

Table 1 Optimization of the reaction conditions[a]

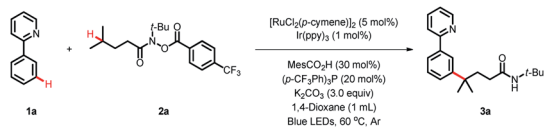

Entry	Deviation from standard condition	Yield[b] (%)
1	None	84
2	No (*p*-CF_3Ph)$_3$P	<10
3	No $MesCO_2H$	65
4	4CzIPN instead of Ir(ppy)$_3$	0
5	Eosin instead of Ir(ppy)$_3$	0
6	[Ir] instead of Ir(ppy)$_3$	0
7	DME as solvent	40
8	DMSO as solvent	Trace
9	DMF as solvent	Trace
10	PhMe as solvent	19
11	$Ru_3(CO)_{12}$ instead of [Ru]	<10
12	$RuCl_3$ instead of [Ru]	Trace
13	No [Ru]	0
14	No Ir(ppy)$_3$	0
15	No light (100 °C)	0

[a] Reaction conditions: **1a** (0.2 mmol), **2a** (0.5 mmol, 2.5 equiv), [$RuCl_2$(*p*-cymene)]$_2$ (5 mol%), Ir(ppy)$_3$ (1 mol%), $MesCO_2H$ (30 mol%), (*p*-CF_3Ph)$_3$P (20 mol%), K_2CO_3 (3.0 equiv), 1,4-dioxane (1.0 mL), blue LEDs, 60 °C, Ar, 36 h. [b] Isolated yield. [Ir] = Ir[dF(CF_3)ppy]$_2$(dtbbpy)PF_6, [Ru] = [$RuCl_2$(*p*-cymene)]$_2$.

other catalysts tested (entries 1, 11 and 12). Control experiments verified the essential roles of the photocatalyst, Ru-catalyst and light (entries 13–15).

With the optimized reaction conditions established, we explored the versatility of this reaction. The scope of 2-phenylpyridines was first investigated using substrate **2a** as a characteristic counterpart (Scheme 2). A wide range of synthetically useful functional groups on the arenes were well tolerated and delivered the C(sp^3)–H/C(sp^2)–H bond coupling products in moderate to high yields. Substrates bearing electron-neutral/electron-donating substituent groups at the *para*-position of aromatic rings proceeded well with **2a** (**3a–3d**, 80–89%). Indeed, electrophilic functional groups, such as a valuable ester substituent, a carbonyl substituent and halides (F, Cl and Br), were well tolerated under these reaction conditions (**3e–3j**, 59–82%). Although the process by which ruthenium participated in the C–H activation approach may be shut down by the steric encumbrance of *ortho*-substituted phenylpyridines, this coupling reaction could also proceed in moderate yields when substituents such as F and OMe were at the *ortho*-position on phenylpyridines (**3k**, 71%; **3l**, 48%; **3o**, 75%). The scope of *meta*-substituted phenylpyridines was more limited, but with small groups such as F and OMe, the coupling reaction could also furnish the corresponding products in moderate yields (**3m**, 45%; **3n**, 37%). With various substituents on the pyridyl, the desired products were obtained in high yields (**3p–3u**, 81–90%). We observed that with other types of directing groups, such as pyrimidine-, pyrazole-, and oxazoline-, the reaction delivered the desired products in moderate to good yields (**3v–3y**, 76–87%; **3ac**, 57%). It is worth noting that when the bioactive purine derivative was used as the directing group, the corresponding product **3z** was obtained in 89% yield. More appealingly, we observed that highly reactive bioactive nucleosides, even those substrates bearing sensitive protecting groups, were all well tolerated and generated the regioselective C(sp^2)–H/C(sp^3)–H bond coupling products **3aa** and **3ab** in 73% and 64% yields, respectively. However, the reaction could not proceed when benzothiazole was used as the directing group (**3ad**, 0). A gram-scale reaction was also conducted. When this transformation was performed at the 5.0 mmol scale using 0.5 mol% $Ir(ppy)_3$, the product **3a** could be obtained in 71% yield upon isolation (1.16 g). The structures of **3n**, **3w** and **3z** were identified unambiguously by X-ray diffraction.

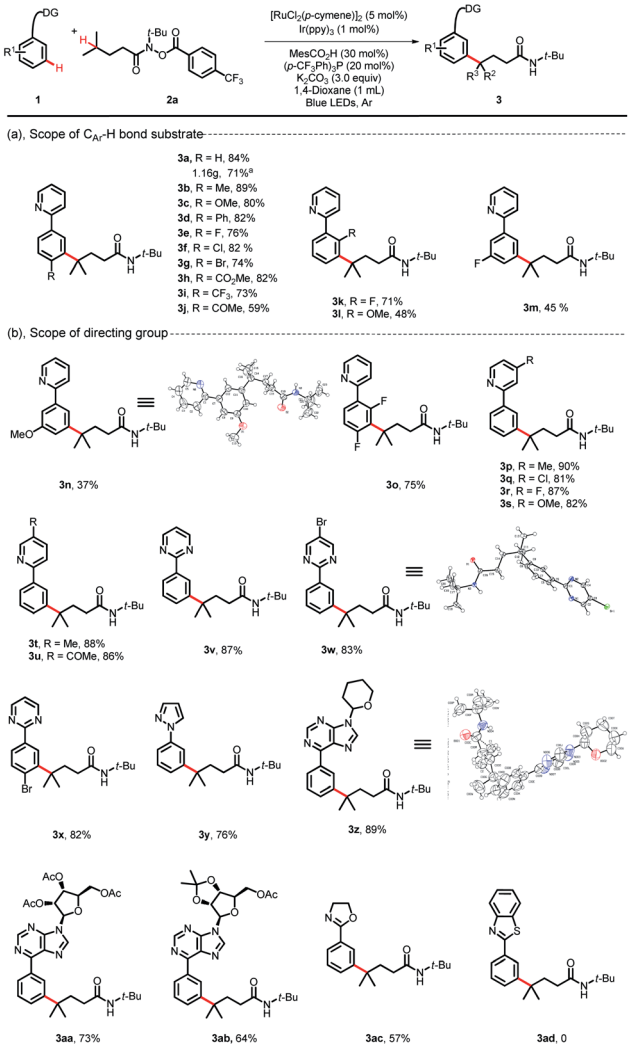

Scheme 2 Substrate scope of the arenes. Reaction conditions: **1** (0.2 mmol), **2a** (0.5 mmol, 2.5 equiv), $[RuCl_2(p\text{-cymene})]_2$ (5 mol%), $Ir(ppy)_3$ (1 mol%), $MesCO_2H$ (30 mol%), $(p\text{-}CF_3Ph)_3P$ (20 mol%), K_2CO_3 (3.0 equiv), 1,4-dioxane (1 mL), blue LEDs, 60 °C, Ar, 36 h, isolated yield. [a]Gram-scale reaction, $Ir(ppy)_3$ (0.5 mol%) for 48 h.

The scope of the hydroxamide compounds was then investigated using 2-phenylpyridine (**1a**) as the coupling partner (Scheme 3). Hydroxamide compounds bearing γ-tertiary C(sp^3)–H bonds were well tolerated and furnished the desired products in good yields (**3ae–3al**, 70–89%). The coupling reaction could also proceed using hydroxamide compounds with secondary C(sp^3)–H bonds at the γ-position, and the γ-arylated products were obtained in moderate to good yields. Substrates bearing diverse chain lengths showed considerable compatibility, and only γ-arylated products were obtained, revealing that the 1,5-HAT process was dominant (**3am–3ap**, 57–71%). Hydroxamide derivatives bearing various functional groups, such as a double bond, halides and esters, could also react with **1a** and deliver the coupling products in moderate yields (**3aq–3as**, 48–54%). The γ-C(sp^3)–H bond next to the oxygen atom could serve as an appropriate coupling partner, giving the product **3av** in 27% yield. For reactions with δ-benzylic or tertiary C(sp^3)–H bonds, the 1,6-HAT products were detected, giving products **3ay** and **3az** in 57% and 62% yields, and the ratios of 1,5-HAT products and 1,6-HAT products were 3.4 : 1 and 4.0 : 1, respectively. The protocol was also applicable to hydroxamide compounds with the γ-primary C(sp^3)–H bond, providing the desired product **3ba** in 22% yield. Late-stage functionalization of natural product derivatives was also conducted, as verified by lithocholic acid, and the corresponding product **3bb** was obtained in 48% yield.

To gain more insight into the reaction mechanism, various control experiments were conducted. First, the reaction was completely inhibited when radical scavengers, such as 1,4-benzoquinone, butylated hydroxytoluene (BHT) or 2,2,6,6-tetramethyl-1-piperidinyloxy (TEMPO), were added, indicating

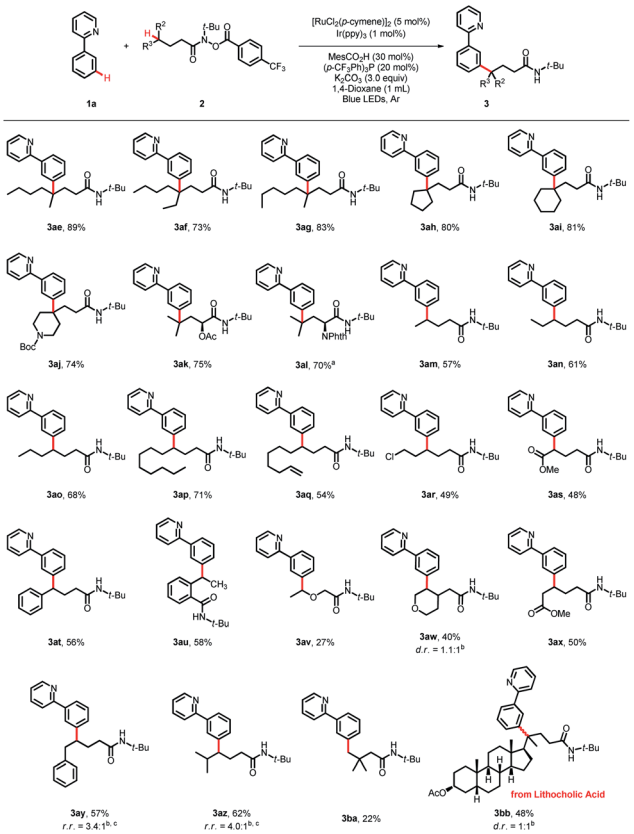

Scheme 3 Substrate scope of the hydroxamide compounds. Reaction conditions: **1a** (0.2 mmol), **2** (0.5 mmol, 2.5 equiv), $[RuCl_2(p\text{-cymene})]_2$ (5 mol%), $Ir(ppy)_3$ (1 mol%), $MesCO_2H$ (30 mol%), $(p\text{-}CF_3Ph)_3P$ (20 mol%), K_2CO_3 (3.0 equiv), 1,4-dioxane (1 mL), blue LEDs, 60 °C, Ar, 36 h, isolated yield. [a]$Ir(ppy)_3$ (2 mol%) for 5 days. [b]Determined by ^1H NMR. [c]The ratio of 1.5-HAT and 1,6-HAT products.

that this coupling reaction presumably proceeded *via* a radical pathway (Scheme 4a). Second, radical clock experiments were also carried out to probe the generation of the C-centered radical. The olefin **4** with a cyclopropyl moiety next to a double bond, which would rearrange in a radical reaction, was found to open under the reaction conditions, producing the corresponding ring closure product **5** in 20% yield (Scheme 4b). These radical-trap experiments verified that a radical pathway was involved in this coupling reaction. Furthermore, when the pre-synthesized cycloruthenated complex **6** was used as the catalyst instead of $[RuCl_2(p\text{-cymene})]_2$, it was found to be an efficient catalyst (Scheme 5a). Likewise, when other types of ruthenium complexes, for example, $Ru(MesCO_2)_2(p\text{-cymene})$ and carboxylate-free ruthenium(II) phosphine complex **7**, were used as catalysts, the reaction proceeded well (Scheme 5b and c). All of these reactions proceeded poorly in the absence of $(p\text{-}CF_3Ph)_3P$; in contrast, the reaction could still occur without $MesCO_2H$, demonstrating that the phosphine ligand played a decisive role in this reaction and that the carboxylate assistance acted as a coaccelerator (Scheme 5). Notably, isotopic labeling experiments were also conducted to explore the possible *ortho*-C–H bond cyclometalation of the arenes. When D_2O was added to the reaction, significant H/D scrambling was observed in the *ortho*-position of arenes (Scheme 6a). In addition, when the isotopically labeled derivative $[D_5]$-**1a** was employed under the standard conditions, it was found that the

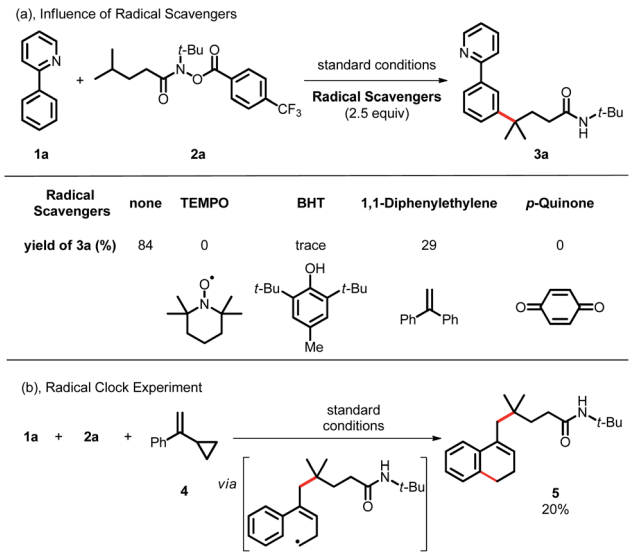

Scheme 4 Radical process experiments.

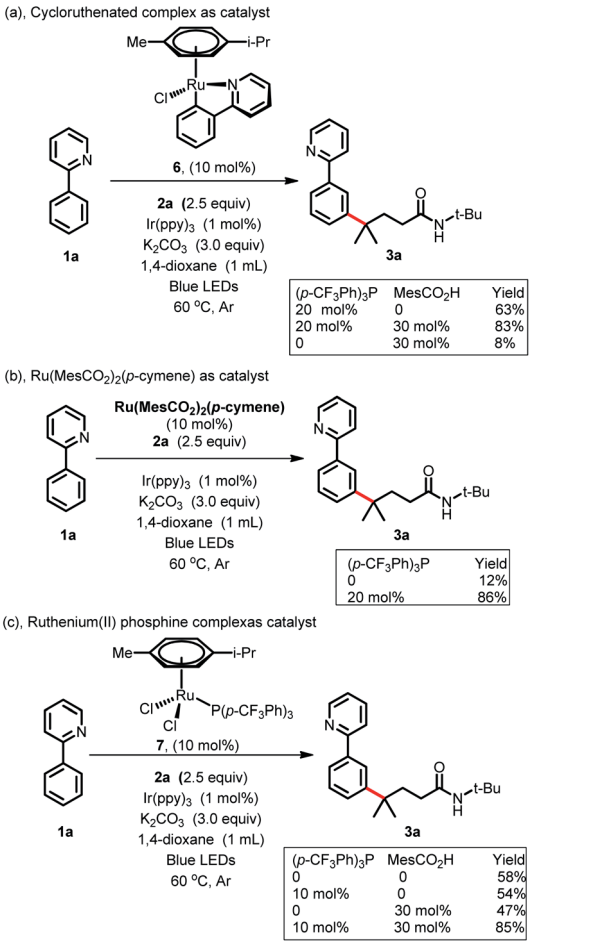

Scheme 5 Control experiments of the Ru-catalyst.

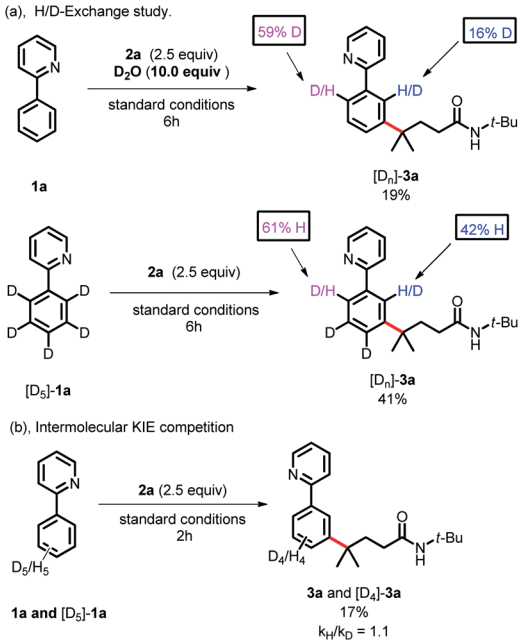

Scheme 6 Mechanistic studies by isotopic labeling experiments.

desired product exhibited obvious H/D scrambling (Scheme 6a). Clearly, different degrees of H/D scrambling in each *ortho*-position of the arenes provided evidence for the remote C(sp^2)–H bond functionalization of arenes occurring at the position *para* to the C–Ru bonds. Intermolecular kinetic isotope effects using substrates **1a** and [D_5]-**1a** indicated that the C(sp^2)–H bond cleavage process at the *ortho*-position of arenes was not kinetically relevant (Scheme 6b).

Furthermore, a luminescence quenching experiment revealed that the hydroxamide **2a** could efficiently quench the excited-state photocatalyst Ir(III)* (Fig. S1†). In addition, cyclic voltammetry studies showed that the reduction potential of **2a** was −1.56 V (*vs.* SCE) in MeCN (Fig. S2†), thus indicating that **2a** can be easily reduced by the excited-state photocatalyst Ir(III)* ($E_{1/2}^{IV/*III} = -1.73$ V *vs.* SCE).

To explain the site-selectivity of the C(sp^2)–C(sp^3) bond formation, Fukui indices were calculated by density functional theory (DFT). The relative Fukui indices for possible Ru(II) intermediates **A–D** and Ru(III) intermediates **E–H** are shown in Scheme 7. On the whole, the relative Fukui indices of the Ru(III) complexes were generally better than those of Ru(II) complexes. This result agreed with previous theoretical and experimental studies that Ru(III) intermediates may be the key intermediates in *meta*-C(sp^2)–H bond functionalization reactions. Then, the products of Ru(III) intermediates in this reaction were investigated. Considering that the Ru(II) complex was used as the catalyst and the Ir(IV) complex could form in our experiments, whether Ru(III) complexes could generate during the redox reaction was assessed by reaction Gibbs free energies (Scheme 8). The calculated results of the Gibbs free energy profile for the redox reaction between Ru(II)/Ir(IV) and Ru(III)/Ir(III) were negative ($\Delta G < 0$), indicating that the possibly formed Ru(II) intermediates in this reaction could be easily oxidized to Ru(III)

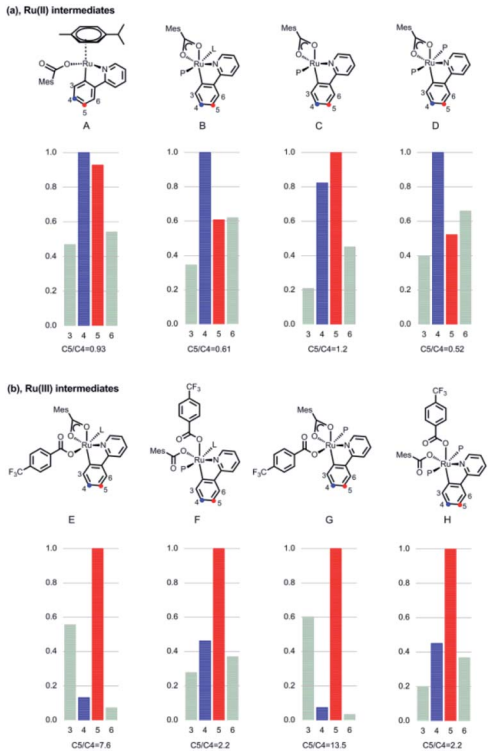

Scheme 7 Calculated Fukui indices of Ru(II)/Ru(III) intermediates. [a]L = 1,4-dioxane, P = PPh_3.

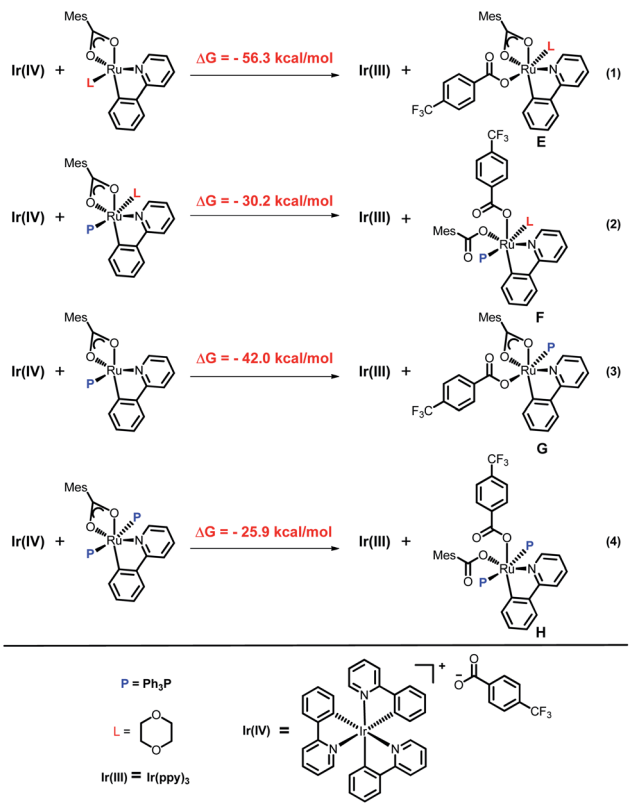

Scheme 8 Calculated Gibbs free energy profile for the redox reaction between Ru(II)/Ir(IV) and Ru(III)/Ir(III).

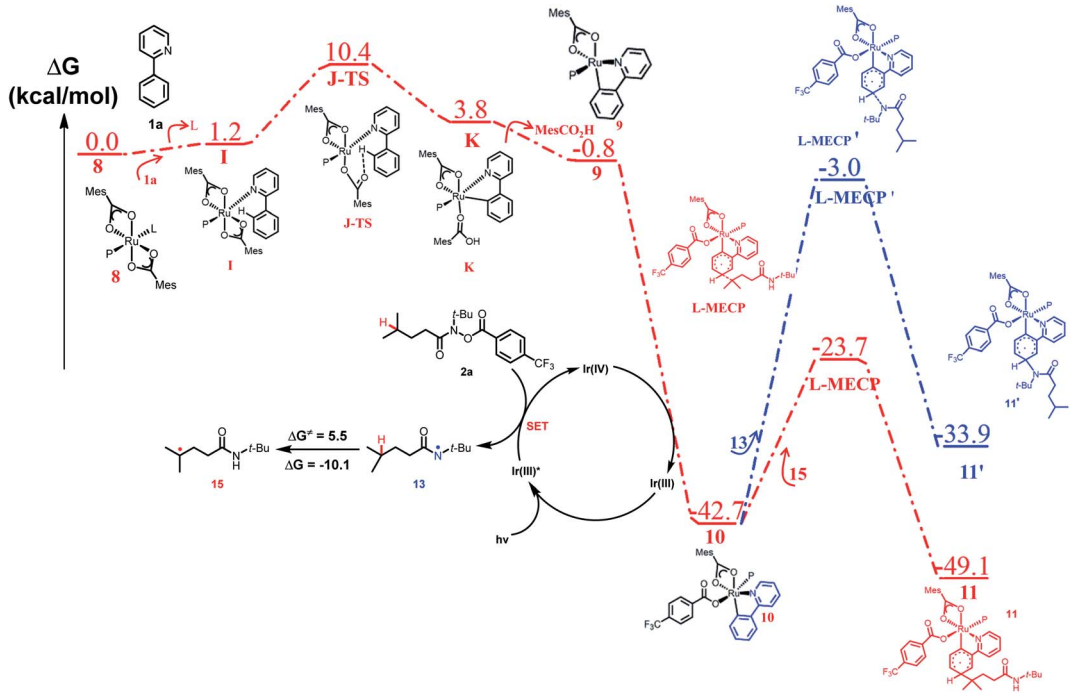

Scheme 9 Computed free energy profile of site-selective coupling of unactivated C(sp^3)–H/*meta*-C(sp^2)–H bonds.

complexes by the Ir(IV) complex. All of these results demonstrated that Ru(III) complexes were generated in this reaction and played the key role in site-selectivity of this reaction. On the basis of the above results, Ru(III) complex **G** was chosen as the reaction intermediate in the following calculated reaction mechanism (Scheme 9). The catalytically active Ru(II) complex **8** transformed into **I** by the ligand exchange, and the Gibbs free energy change of this step was only 1.2 kcal mol^{-1}. Next, the intermediate **K** was formed by the $MesCOO^-$ assisted C–H bond activation process from **I** *via* **J-TS** with an energy barrier of 9.2 kcal mol^{-1}, and was 3.8 kcal mol^{-1} compared with **8**. Then, $MesCO_2H$ left forming intermediate **9** and the energy decreased to −0.8 kcal mol^{-1} by the entropy effect. Subsequently, the Ru(II) intermediate **9** was oxidized to Ru(III) intermediate **10** by the Ir(IV) complex resulting from single electron transfer (SET) from Ir(ppy)* to **2a**, releasing about 42 kcal mol^{-1}. Finally, the alkyl radical **15** underwent addition to the benzene ring of **10** to form **11** through **L-MECP** with an energy barrier of 19.0 kcal mol^{-1}, releasing 6.4 kcal mol^{-1} energy. In contrast, the nitrogen-centered radical **13** underwent addition to the same site through **L-MECP′** with an energy barrier of 39.7 kcal mol^{-1} to form **11′**. In addition, N-centered radical **13** could easily transform to C-centered radical **15** through intramolecular 1,5-HAT with an energy barrier of only 5.5 kcal mol^{-1}. Hence, the intermediate **11** was dominant, and the calculated results were consistent with the experimental results that no *meta* aminated arenes were observed. After that, **11** underwent the LMCT step, rearomatization and demetalation to form the *meta*-alkylated arenes, which has been reported by previous reports. The computational results implied that the reaction mechanism was plausible under our reaction conditions.

Based on the previous reports,[11a,17b-d] DFT calculations and control experiments, a plausible mechanism was proposed for this coupling reaction as depicted in Scheme 10. SET from the photoexcited $Ir(ppy)_3$ catalyst (Ir(III)*) to the hydroxamide substrate **2a** and subsequent N–O bond cleavage generated the nitrogen-centered radical **13** and Ir(IV). Then, intramolecular 1,5-HAT of **13** occurred, forming the carbon-centered radical **15**. The cyclometalated Ru(II) complex **9** formed from the reversible

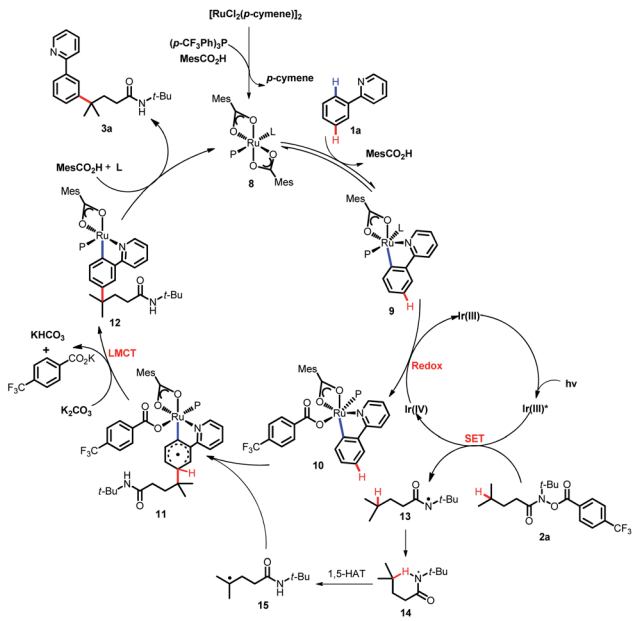

Scheme 10 Proposed mechanism.

carboxylate-assisted C–H bond ruthenation of the arene was then oxidized by the formed Ir(IV) complex to produce a Ru(III) complex **10**, and regenerated the $Ir(ppy)_3$ catalyst simultaneously. The formed carbon-centered radical **15** underwent C_{Ar}–H bond addition at the position *para* to the C–Ru(III) bond of Ru(III) complex **10**, generating the species **11**, which underwent subsequent rearomatization *via* the LMCT step to afford the Ru(II) complex **12**. Eventually, the anticipated coupling product **3a** was delivered by demetalation, and the catalytically active ruthenium(II) complex **8** was regenerated.

Conclusions

In conclusion, we developed a novel example of metallaphotoredox-enabled regioselective CDC of dual remote C–H bonds, including unactivated γ-C(sp^3)–H bonds in amides and *meta*-C(sp^2)–H bonds in arenes, to construct challenging *meta*-alkylated arenes. This reaction represented a novel case of employing Ru/photoredox dual catalysis for regioselective coupling of unactivated C(sp^3)–H bonds in amides and C(sp^2)–H bonds arenes *via* a new catalytic process, and provided a new strategy to synthesize *meta*-functionalized arenes under mild reaction conditions. The reaction worked well with primary, secondary and tertiary C(sp^3)–H bonds in amides and a broad range of arenes were well tolerated. Moreover, excellent regioselectivity was observed in terms of inert C(sp^3)–H bonds in hydroxamides and *meta*-C(sp^2)–H bonds in arenes. Detailed mechanistic studies, including DFT calculations and control experiments, explained the high regioselectivity of C(sp^3)–H bonds and C(sp^2)–H bonds, and provided a theoretical basis for this site-selective coupling reaction.

Data availability

Detailed synthetic procedures, and complete characterization data for all new compounds can be found in the ESI.†

Author contributions

Methodology, H.-C. L. and X. K.; investigation, H.-C. L. and X. K.; writing original draft, H.-C. L. and X. K; writing review & editing, X.-P. G., Y. L., Z.-J. N., X.-Y. G., X.-S. L., Y.-Z. W., W.-Y. S., Y.-C. H., X.-Y. L., and Y.-M. L.; Y. L. is responsible for the calculation studies; funding acquisition, Y.-M. L.; supervision, Y.-M. L. All authors co-wrote the paper, discussed the results, analyzed the data and commented on the paper.

Conflicts of interest

The authors declare no competing interests.

Acknowledgements

We thank the National Natural Science Foundation of China (NSF 22171114 and 21772075) and Henan Key Scientific Research Projects (22A150001) for support.

Notes and references

1 (*a*) W. Xie, D. Kim and S. Chang, *J. Am. Chem. Soc.*, 2020, **142**, 20588–20593; (*b*) X. Wang, D. Leow and J.-Q. Yu, *J. Am. Chem. Soc.*, 2011, **133**, 13864–13867; (*c*) H. Wang, X. Gao, Z. Lv, T. Abdelilah and A. Lei, *Chem. Rev.*, 2019, **119**, 6769–6787; (*d*) N. Kuhl, M. N. Hopkinson, J. Wencel-Delord and F. Glorius, *Angew. Chem., Int. Ed.*, 2012, **51**, 10236–10254; (*e*) S. A. Girard, T. Knauber and C.-J. Li, *Angew. Chem., Int. Ed.*, 2014, **53**, 74–100.

2 D. R. Stuart and K. Fagnou, *Science*, 2007, **316**, 1172.

3 (*a*) B.-J. Li, S.-L. Tian, Z. Fang and Z.-J. Shi, *Angew. Chem., Int. Ed.*, 2008, **47**, 1115–1118; (*b*) T. W. Lyons, K. L. Hull and M. S. Sanford, *J. Am. Chem. Soc.*, 2011, **133**, 4455–4464; (*c*) X. Zhao, C. S. Yeung and V. M. Dong, *J. Am. Chem. Soc.*, 2010, **132**, 5837–5844; (*d*) Y. Yang, J. Lan and J. You, *Chem. Rev.*, 2017, **117**, 8787–8863.

4 G. Deng, L. Zhao and C.-J. Li, *Angew. Chem., Int. Ed.*, 2008, **47**, 6278–6282.

5 (*a*) G. Li, D. Li, J. Zhang, D.-Q. Shi and Y. Zhao, *ACS Catal.*, 2017, **7**, 4138–4143; (*b*) Y.-Z. Li, B.-J. Li, X.-Y. Lu, S. Lin and Z.-J. Shi, *Angew. Chem., Int. Ed.*, 2009, **48**, 3817–3820; (*c*) S. R. Neufeldt and M. S. Sanford, *Acc. Chem. Res.*, 2012, **45**, 936–946.

6 (*a*) S. J. Blanksb and G. B. Ellison, *Acc. Chem. Res.*, 2003, **36**, 255–263; (*b*) T. Newhouse and P. S. Baran, *Angew. Chem., Int. Ed.*, 2011, **50**, 3362–3374.

7 (*a*) A. W. Hofmann, *Ber. Dtsch. Chem. Ges.*, 1883, **16**, 558–560; (*b*) R. S. Neale, *Synthesis*, 1971, **1971**, 1–15; (*c*) M. E. Wolff, *Chem. Rev.*, 1963, **63**, 55–64; (*d*) S. Z. Zard, *Chem. Soc. Rev.*, 2008, **37**, 1603–1618.

8 (*a*) J. C. K. Chu and T. Rovis, *Angew. Chem., Int. Ed.*, 2018, **57**, 62–101; (*b*) B. J. Groendyke, D. I. AbuSalim and S. P. Cook, *J. Am. Chem. Soc.*, 2016, **138**, 12771–12774; (*c*) W. Guo, Q. Wang and J. Zhu, *Chem. Soc. Rev.*, 2021, **50**, 7359–7377; (*d*) E. Nobile, T. Castanheiro and T. Besset, *Angew. Chem., Int. Ed.*, 2021, **60**, 12170–12191; (*e*) A. F. Prusinowski, R. K. Twumasi, E. A. Wappes and D. A. Nagib, *J. Am. Chem. Soc.*, 2020, **142**, 5429–5438; (*f*) N. Radhoff and A. Studer, *Angew. Chem., Int. Ed.*, 2021, **60**, 3561–3565; (*g*) S. M. Rafferty, J. E. Rutherford, L. Zhang, L. Wang and D. A. Nagib, *J. Am. Chem. Soc.*, 2021, **143**, 5622–5628; (*h*) E. Tsui, H. Wang and R. R. Knowles, *Chem. Sci.*, 2020, **11**, 11124–11141; (*i*) L. Wang, Y. Xia, V. Derdau and A. Studer, *Angew. Chem., Int. Ed.*, 2021, **60**, 18645–18650; (*j*) Y. Xia, K. Jana and A. Studer, *Chem. - Eur. J.*, 2021, **27**, 16621–16625; (*k*) L. M. Stateman, K. M. Nakafuku and D. A. Nagib, *Synthesis*, 2018, **50**, 1569–1586.

9 (*a*) A. N. Herron, D. Liu, G. Xia and J.-Q. Yu, *J. Am. Chem. Soc.*, 2020, **142**, 2766–2770; (*b*) S. P. Morcillo, E. M. Dauncey, J. H. Kim, J. J. Douglas, N. S. Sheikh and D. Leonori, *Angew. Chem., Int. Ed.*, 2018, **57**, 12945–12949; (*c*) S. M. Thullen, S. M. Treacy and T. Rovis, *J. Am. Chem. Soc.*, 2019, **141**, 14062–14067; (*d*) Y. Xia, L. Wang and A. Studer, *Angew. Chem., Int. Ed.*, 2018, **57**, 12940–12944.

10 (*a*) D.-F. Chen, J. C. K. Chu and T. Rovis, *J. Am. Chem. Soc.*, 2017, **139**, 14897–14900; (*b*) G. J. Choi, Q. Zhu, D. C. Miller,

C. J. Gu and R. R. Knowles, *Nature*, 2016, **539**, 268–271; (*c*) W.-J. Yue, C. S. Day and R. Martin, *J. Am. Chem. Soc.*, 2021, **143**, 6395–6400.

11 (*a*) H. Chen, W. Fan, X.-A. Yuan and S. Yu, *Nat. Commun.*, 2019, **10**, 4743; (*b*) N. Kim, C. Lee, T. Kim and S. Hong, *Org. Lett.*, 2019, **21**, 9719–9723; (*c*) G.-X. Li, X. Hu, G. He and G. Chen, *Chem. Sci.*, 2019, **10**, 688–693.

12 (*a*) X. Zeng, W. Yan, M. Paeth, S. B. Zacate, P.-H. Hong, Y. Wang, D. Yang, K. Yang, T. Yan, C. Song, Z. Cao, M.-J. Cheng and W. Liu, *J. Am. Chem. Soc.*, 2019, **141**, 19941–19949; (*b*) A. Modak, E. N. Pinter and S. P. Cook, *J. Am. Chem. Soc.*, 2019, **141**, 18405–18410; (*c*) Z. Li, Q. Wang and J. Zhu, *Angew. Chem., Int. Ed.*, 2018, **57**, 13288–13292.

13 (*a*) U. Dutta, S. Maiti, T. Bhattacharya and D. Maiti, *Science*, 2021, **372**, eabd5992; (*b*) J. A. Leitch and C. G. Frost, *Chem. Soc. Rev.*, 2017, **46**, 7145–7153; (*c*) J. Li, S. De Sarkar and L. Ackermann, *Meta-* and *para*-Selective C–H Functionalization by C–H Activation, in *C–H Bond Activation and Catalytic Functionalization*, ed. I. Dixneuf, H. Pierre and H. Doucet, Springer International Publishing, Cham, 2016, pp. 217–257.

14 C. J. Teskey, A. Y. W. Lui and M. F. Greaney, *Angew. Chem., Int. Ed.*, 2015, **54**, 11677–11680.

15 O. Saidi, J. Marafie, A. E. W. Ledger, P. M. Liu, M. F. Mahon, G. Kociok-Köhn, M. K. Whittlesey and C. G. Frost, *J. Am. Chem. Soc.*, 2011, **133**, 19298–19301.

16 Z. Fan, J. Ni and A. Zhang, *J. Am. Chem. Soc.*, 2016, **138**, 8470–8475.

17 (*a*) P. Gandeepan, J. Koeller, K. Korvorapun, J. Mohr and L. Ackermann, *Angew. Chem., Int. Ed.*, 2019, **58**, 9820–9825; (*b*) N. Hofmann and L. Ackermann, *J. Am. Chem. Soc.*, 2013, **135**, 5877–5884; (*c*) K. Korvorapun, R. Kuniyil and L. Ackermann, *ACS Catal.*, 2020, **10**, 435–440; (*d*) J. Li, S. Warratz, D. Zell, S. De Sarkar, E. E. Ishikawa and L. Ackermann, *J. Am. Chem. Soc.*, 2015, **137**, 13894–13901; (*e*) Z. Ruan, S.-K. Zhang, C. Zhu, P. N. Ruth, D. Stalke and L. Ackermann, *Angew. Chem., Int. Ed.*, 2017, **56**, 2045–2049; (*f*) A. Sagadevan and M. F. Greaney, *Angew. Chem., Int. Ed.*, 2019, **58**, 9826–9830.

18 (*a*) X.-G. Wang, Y. Li, H.-C. Liu, B.-S. Zhang, X.-Y. Gou, Q. Wang, J.-W. Ma and Y.-M. Liang, *J. Am. Chem. Soc.*, 2019, **141**, 13914–13922; (*b*) X.-Y. Gou, Y. Li, Y.-Y. Luan, W.-Y. Shi, C.-T. Wang, Y. An, B.-S. Zhang and Y.-M. Liang, *ACS Catal.*, 2021, **11**, 4263–4270.

19 H.-C. Liu, Y. Li, X.-P. Gong, Z.-J. Niu, Y.-Z. Wang, M. Li, W.-Y. Shi, Z. Zhang and Y.-M. Liang, *Org. Lett.*, 2021, **23**, 2693–2698.